[10] Higashiyama M, Doi O, Kodama K, Yokouchi H, Imaoka S, Koyama H. Surgical treatment of adrenal metastasis following pulmonary resection for lung cancer: comparison of adrenalectomy with palliative therapy. Int Surg 1994;79:124–9.
[11] Kebebew E, Siperstein AE, Clark OH, Duh QY. Results of laparoscopic adrenalectomy for suspected and unsuspected malignant adrenal neoplasms. Arch Surg 2002;137:948–51.
[12] Kim SH, Brennan MF, Russo P, Burt ME, Coit DG. The role of surgery in the treatment of clinically isolated adrenal metastasis. Cancer 1998;82:389–94.
[13] Linos DA, Stylopoulos N, Boukis M, Souvatzoglou A, Raptis S, Papadimitriou J. Anterior, posterior, or laparoscopic approach for the management of adrenal diseases? Am J Surg 1997;173:120–5.
[14] Mercier O, Fadel E, de Perrot M, et al. Surgical treatment of solitary adrenal metastasis from non-small cell lung cancer. J Thorac Cardiovasc Surg 2005;130:136–40.
[15] Moinzadeh A, Gill IS. Laparoscopic radical adrenalectomy for malignancy in 31 patients. J Urol 2005;173:519–25.
[16] Porte H, Siat J, Guibert B, et al. Resection of adrenal metastases from non-small cell lung cancer: a multicenter study. Ann Thorac Surg 2001;71:981–5.
[17] Sarela AI, Murphy I, Coit DG, Conlon KC. Metastasis to the adrenal gland: the emerging role laparoscopic surgery. Ann Surg Oncol 2003;10:1191–6.
[18] Schell SR, Talamini MA, Udelsman R. Laparoscopic adrenalectomy for nonmalignant disease: improved safety, morbidity, and cost-effectiveness. Surg Endosc 1999;13:30–4.
[19] Sebag F, Calzolari F, Harding J, Sierra M, Palazzo FF, Henry JF. Isolated adrenal metastasis: the role of laparoscopic surgery. World J Surg 2006;30:888–92.
[20] Seppenwoolde Y, Shirato H, Kitamura K, et al. Precise and real-time measurement of 3D tumor motion in lung due to breathing and heartbeat, measured during radiotherapy. Int J Radiat Oncol Biol Phys 2002;53:822–34.
[21] Shirato H, Shimizu S, Kitamura K, et al. Four-dimensional treatment planning and fluoroscopic real-time tumor tracking radiotherapy for moving tumor. Int J Radiat Oncol Biol Phys 2000;48:435–42.
[22] Shirato H, Shimizu S, Kunieda T, et al. Physical aspects of a real-time tumor tracking system for gated radiotherapy. Int J Radiat Oncol Biol Phys 2000;48:1187–95.
[23] Shirato H, Shimizu S, Shimizu T, Nishioka T, Miyasaka K. Real-time tumour tracking radiotherapy. Lancet 1999;353:1331–2.
[24] Shirato H, Suzuki K, Sharp GC, et al. Speed and amplitude of lung tumor motion precisely detected in four-dimensional setup and in real-time tumor-tracking radiotherapy. Int J Radiat Oncol Biol Phys 2006;64:1229–36.
[25] Soffen EM, Solin LJ, Rubenstein JH, Hanks GE. Palliative radiotherapy for symptomatic adrenal metastases. Cancer 1990;65:1318–20.
[26] Suzuki K, Ushiyama T, Mugiya S, Kageyama S, Saisu K, Fujita K. Hazards of laparoscopic adrenalectomy in patients with adrenal malignancy. J Urol 1997;158:2227.
[27] Taguchi H, Sakuhara Y, Hige S, et al. Intercepting radiotherapy using a real-time tumor-tracking radiotherapy system for highly selected patients with hepatocellular carcinoma unresectable with other modalities. Int J Radiat Oncol Biol Phys 2007;69:376–80.
[28] Therasse P, Arbuck SG, Eisenhauer EA, et al. New guidelines to evaluate the response to treatment in solid tumors. European Organization for Research and Treatment of Cancer, National Cancer Institute of the United States, National Cancer Institute of Canada. J Natl Cancer Inst 2000;92:205–16.
[29] van Sörnsen de Koste JR, Senan S, Kleynen CE, Slotman BJ, Lagerwaard FJ. Renal mobility during uncoached quiet respiration: an analysis of 4DCT scans. Int J Radiat Oncol Biol Phys 2006;64:799–803.
[30] Wells SA, Merke DP, Cutler GB, Norton JA, Lacroix A. Therapeutic controversy: the role of laparoscopic surgery in adrenal disease. J Clin Endocrinol Metab 1998;83:3041–9.
[31] Zeng ZC, Tang ZY, Fan J, et al. Radiation therapy for adrenal gland metastases from hepatocellular carcinoma. Jpn J Clin Oncol 2005;35:61–7.

Int. J. Radiation Oncology Biol. Phys., Vol. ■, No. ■, pp. 1–5, 2009

0360-3016/09/$–see front matter

ELSEVIER

doi:10.1016/j.ijrobp.2008.11.026

CLINICAL INVESTIGATION

CLINICAL OUTCOMES OF STEREOTACTIC BODY RADIOTHERAPY FOR SMALL LUNG LESIONS CLINICALLY DIAGNOSED AS PRIMARY LUNG CANCER ON RADIOLOGIC EXAMINATION

TETSUYA INOUE, M.D.,* SHINICHI SHIMIZU, M.D.,* RIKIYA ONIMARU, M.D.,* ATSUYA TAKEDA, M.D.,† HIROSHI ONISHI, M.D.,‡ YASUSHI NAGATA, M.D.,§ TOMOKI KIMURA, M.D.,‖ KATSUYUKI KARASAWA, M.D.,¶ TAKURO ARIMOTO, M.D.,# MASATO HAREYAMA, M.D.,** EIKI KIKUCHI, M.D.,†† AND HIROKI SHIRATO, M.D.*

*Hokkaido University Department of Radiology, Sapporo, Japan; †Ofuna Central Hospital, Department of Radiology, Ofuna, Japan; ‡Yamanashi University Department of Radiology, Kofu, Japan; §Hiroshima University Department of Radiology, Hiroshima, Japan; ‖Kagawa University Department of Radiology, Takamatsu, Japan; ¶Tokyo Metropolitan Komagome Hospital, Department of Radiology, Tokyo, Japan; #Kitami Red Cross Hospital, Department of Radiology, Kitami, Japan; **Sapporo Medical University Department of Radiology, Sapporo, Japan; and ††Hokkaido University First Department of Internal Medicine, Sapporo, Japan

Purpose: Image-guided biopsy occasionally fails to diagnose small lung lesions, which are highly suggestive of primary lung cancer. The aim of the present study was to evaluate the outcome of stereotactic body radiotherapy (SBRT) for small lung lesions that were clinically diagnosed as primary lung cancer without pathologic confirmation.
Methods and Materials: A total of 115 patients were treated with SBRT in 12 institutions. Tumor size ranged from 5 to 45 mm in diameter, with a median of 20 mm.
Results: The 3-year and 5-year overall survival rates for patients with a tumor size ≤20 mm in diameter ($n = 58$) were both 89.8%, compared with 60.7% and 53.1% for patients with tumors >20 mm ($n = 57$) ($p < 0.0005$), respectively. Local progression occurred in 2 patients (3.4%) with a tumor size ≤20 mm and in 3 patients (5.3%) with tumors >20 mm. Among the patients with a tumor size ≤20 mm, Grade 2 pulmonary complications were observed in 2 (3.4%), but no Grade 3 to 5 toxicity was observed. In patients with a tumor size >20 mm, Grades 2, 3, and 5 toxicity were observed in 5 patients (8.8%), 3 patients (5.3%), and 1 patient (1.8%), respectively.
Conclusion: In patients with a tumor ≤20 mm in diameter, SBRT was reasonably safe in this retrospective study. The clinical implications of the high local control rate depend on the accuracy of clinical/radiologic diagnosis for small lung lesions and are to be carefully evaluated in a prospective study. © **2009 Elsevier Inc.**

Lung cancer, Stereotactic radiotherapy, Stereotactic body radiotherapy.

INTRODUCTION

Pathologic diagnosis is essential for the treatment of primary lung cancer. However, image-guided biopsy occasionally fails to diagnose small lung lesions, which are highly suggestive of primary lung cancer. When patients refuse re-biopsy or surgical resection, watchful waiting is usually indicated. There are other groups of patients in whom a pathologic diagnosis is very difficult to make, such as those with medical reasons for not being able to undergo biopsy and those with a history of surgical resection of non–small-cell lung cancer (NSCLC) and a small peripheral lung lesion on follow-up computed tomography (CT). The patients in the latter group often have difficulty undergoing a second surgical resection because of lowered respiratory function resulting from the previous surgery. Patients with cancer who are under watchful waiting are at risk for invasive growth of the primary tumor, lymphatic spread, and distant metastasis. Patients who choose to receive elective surgical resection of the small lung lesions to quantify the pathologic diagnosis may experience serious respiratory dysfunction. A proportion of the patients who do not have malignant tumors are inevitably overtreated and experience surgical complications.

Stereotactic body radiotherapy (SBRT) has been one of the treatments for Stage I NSCLC in medically inoperable patients. Recently, high local control and survival rates of SBRT were

Reprint requests to: Hiroki Shirato, M.D., Ph.D., Department of Radiology, Hokkaido University Graduate School of Medicine, North 15 West 7, Kita-ku, Sapporo 060-8638, Japan. Tel: +81-11-706-5977; Fax: +81-11-706-7876; E-mail: hshirato@radi.med.hokudai.ac.jp

Conflict of interest: none.

Acknowledgment—This study was supported in part by the Ministry of Health, Labour, and Welfare and by the Ministry of Education, Culture, Sports, Science, and Technology, Japan.

Received Aug 21, 2008, and in revised form Nov 17, 2008. Accepted for publication Nov 20, 2008.

reported in several studies (1–7). Onishi *et al.* summarized the results of a Japanese series retrospectively and reported that a pulmonary complication rate of above Grade 2 arose in only 5.4% of patients (1). For the patients who received a dose compatible with the biologic effective dose (BED) of 100 Gy or more, the local control rate was 91.6%. For the patients who were judged to have been operable but who were treated with SBRT, the 5-year overall survival rate was 70.8%, which is equivalent to that achieved in the previously mentioned surgery series (1).

A serious question among radiation oncologists is whether it is ethically justifiable not to give SBRT to those patients who have peripheral lung lesions highly suggestive of lung cancer but who failed to have lung cancer diagnosed pathologically. If SBRT is as safe as image-guided re-biopsy and as effective as surgical resection, it may be ethical to give SBRT to these patients. However, we cannot answer this question, because the risk and benefit have not been compared between elective surgical resection, watchful waiting, and SBRT for small peripheral lung lesions without pathologic confirmation.

We have found in a national survey of SBRT that a small number of patients with the clinical diagnosis of NSCLC are actually treated with SBRT without pathologic confirmation in each institution. The aim of the present study was to evaluate the outcome of SBRT for peripheral small lung lesions that were clinically diagnosed as primary lung cancer without pathologic confirmation in 12 institutions during the past 10 years in Japan.

METHODS AND MATERIALS

Eligibility criteria

Twelve institutions were selected from the member institutions of the Japan Clinical Oncology Group trial, JCOG0403, for which the quality of clinical record and dosimetry accuracy of SBRT had already been evaluated by audit (8). This is a multi-institutional retrospective study using the same eligibility criteria, which were that (a) surgery was contraindicated or refused, (b) the tumor diameter was <50 mm, (c) tumors were highly suggestive of primary lung cancer and diagnosed as Stage I lung cancer clinically but the patients did not have a pathologic diagnosis, and (d) the performance status was 0 to 2 according to World Health Organization guidelines.

Patients

A total of 115 patients who were highly suspected of having lung cancer but who lacked pathologic confirmation of the disease were diagnosed with Stage I lung cancer clinically and treated with SBRT in 12 institutions during the last 10 years in Japan. The patient characteristics are given in Table 1. There were 93 cases of T1N0M0 and 22 cases of T2N0M0 disease. The number of medically operable and inoperable patients was 43 and 72, respectively. Tumor size was recorded at the maximum diameter on the CT scan taken at the start of radiotherapy. The median tumor size was 20 mm (range, 5–45 mm). The median follow-up period was 14 months (range, 1–142 months). There were 11 patients whose follow-up period was <4 months at the time of this analysis.

Diagnosis was based on CT findings and enlargement of the lesion on sequential examination with or without fluorodeoxyglucose (FDG)–positron emission tomography (PET) findings. The tumors were diagnosed as highly suggestive of primary lung cancer by diagnostic radiologists when there was definitive enlargement of the lesion on sequential CT examination and/or positive findings on FDG-PET without any metastatic lesion in the diagnostic evaluation. Several findings such as the configuration of the lung lesion were also used in the diagnosis. Of 72 patients who were examined with FDG-PET, 67 patients had positive findings on FDG-PET. Other clinical history and findings as well as laboratory findings were also used for diagnosis as much as possible to prevent inclusion of patients with metastatic lung tumors or inflammatory or granulomatous lesions in the study population.

Table 1. Characteristics of patients (115 patients)

Characteristic	Value
Age (y)	
Median	77
Range	50–92
Gender (*n*)	
Male	87
Female	28
Tumor size (mm)	
Median	20
Range	5–45
T stage (*n*)	
T1	93
T2	22
Medical condition (*n*)	
Operable	43
Inoperable	72

The reasons for the lack of pathologic confirmation were as follows: (a) bronchoscope- or CT-guided biopsy failed in 59 patients, and these patients refused re-biopsy or surgical resection; (b) 21 patients were not indicated for a biopsy procedure or surgery because of medical complications; (c) 14 patients refused a biopsy procedure as well as surgery even at the initial examination; (d) a biopsy was not indicated in 14 patients because their history of NSCLC was strongly suggestive of the new development of a second primary NSCLC, likely inoperable, and they refused surgery; and (e) a biopsy was not indicated in 7 patients because there was little possibility to confirm the pathology because of the tumor's small size, and these patients refused surgery.

Radiotherapy

All patients underwent irradiation using stereotactic techniques. Three-dimensional treatment planning was performed using non-coplanar static ports or dynamic arcs. Various techniques using breathing control or gating methods and immobilization devices such as a vacuum cushion with or without a stereotactic body frame were used to reduce respiratory internal margins. Appropriate margins were adopted for the clinical target volume and the planning target volume.

A total dose of 30 to 70 Gy at the isocenter was administered in two to 10 fractions. Using a linear-quadratic model, we defined the BED as $nd(1+d/\alpha/\beta)$, with Gray units, where n was the fractionation number, d was the daily dose, and the α/β ratio was assumed to be 10 for tumors. The BED was not corrected with values for tumor doubling time or treatment term. The median BED at the isocenter in this study was 106 Gy (range, 56–141 Gy).

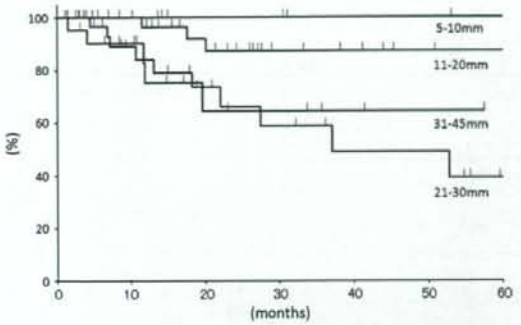

Fig. 1. Kaplan-Meier curve of overall survival rates for the patients with a tumor size (diameter) of 5 to 10 mm ($n = 11$), 11 to 20 mm ($n = 47$), 21 to 30 mm ($n = 35$), and 31 to 45 mm ($n = 22$).

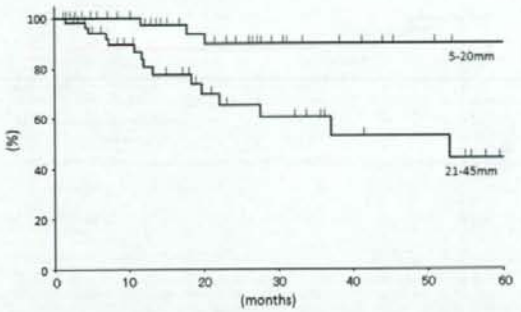

Fig. 2. Kaplan-Meier curve of overall survival rates for the patients with a tumor size (diameter) of 5 to 20 mm ($n = 58$) and 21 to 45 mm ($n = 57$). A statistically significant difference was found ($p < 0.0005$) between the two groups.

Ethical considerations

Use of SBRT was approved for Stage I lung cancer by the ethics committee in each institution. Clinically diagnosed Stage I lung cancer was not included in the ineligibility criteria at each institution. Written informed consent to receive SBRT was obtained from all patients. This retrospective study was approved by the ethics committee of each institution and was performed in accordance with the 1975 Declaration of Helsinki, as revised in 2000.

Statistical analysis

Overall survival rates were calculated from the first day of treatment using the Kaplan-Meier method. The log-rank test was used to calculate statistically significant differences. A value of $p < 0.05$ was considered to be statistically significant.

RESULTS

Survival

We separated the patients into four groups by tumor size at its maximum diameter, consisting of the 5 to 10 mm (Group A; $n = 11$), 11 to 20 mm (Group B; $n = 47$), 21 to 30 mm (Group C; $n = 35$), and 31 to 45 mm (Group D; $n = 22$) groups. The 3-year and 5-year overall survival rates were both 100% for Group A, both 87.2% for Group B, 58.7% and 48.9% for Group C, and both 64.5% for Group D (Fig. 1). When we excluded the 11 patients whose follow-up period was <4 months, there was no apparent difference in these results; 3-year and 5-year overall survival rates were both 100% for Group A, both 87.2% for Group B, and 58.7% and 39.2% for Group C, and both 67.7% for Group D.

The 3-year and 5-year overall survival rates were both 89.8% for patients with a tumor size ≤20 mm ($n = 58$) compared with 60.7% and 53.1% for patients with a tumor size >20 mm ($n = 57$) ($p < 0.0005$; Fig. 2). According to medical operability, the 3-year and 5-year overall survival rates for operable patients ($n = 43$) were both 88.4%, compared with 67.0% and 60.9% for inoperable patients ($n = 72$) (Fig. 3). According to BED, the 3-year and 5-year overall survival rates for the patients with BED <100 Gy ($n = 17$) were both 71.8%, compared with 76.6% and 61.9% for the patients with BED ≥ 100 Gy ($n = 98$) (Fig. 4).

Local tumor response and distant metastases

Local progression occurred in 2 patients (3.4%) with a tumor size ≤20 mm and in 3 patients (5.3%) with a tumor size >20 mm. Lymphatic and distant metastasis were observed in 3 patients (5.2%) and 6 patients (10.3%) with a tumor size ≤20 mm and in 6 patients (10.5%) and 10 patients (17.5%) with a tumor size >20 mm, respectively. For the patients with BED <100 Gy, no local progression occurred.

Toxicities

Pulmonary adverse effects were graded according to the Common Toxicity Criteria for Adverse Events version 3.0. In brief, radiation pneumonitis was graded as follows: Grade 1, asymptomatic, radiologic findings only; Grade 2, symptomatic, not interfering with activities of daily life (ADL); Grade 3, interfering with ADL, O2 indicated; Grade 4, life-threatening, ventilatory support indicated; and Grade 5, death.

Of patients with a tumor size ≤20 mm in diameter, Grade 2 pulmonary complications were observed in 2 patients (3.4%), whereas no patients experienced Grade 3 to 5 toxicities. In patients with a tumor size >20 mm, Grades 2, 3, and 5 pulmonary toxicities were observed in 5 patients (8.8%), 3 patients (5.3%), and 1 patient (1.8%), respectively. A Grade 5 pulmonary complication occurred in 1 patient with interstitial pneumonia, which resulted in acute worsening from SBRT after 1.5 months. One case of radiation pleuritis, one case of intercostal neuralgia, and one case of rib fracture were observed, but these patients' symptoms were controlled easily by conservative treatment. Grade 2 pulmonary toxicity occurred in 3 cases (17.6%) in patients with BED <100 Gy and in 8 cases (8.2%) in patients with BED ≥100 Gy.

DISCUSSION

There is no doubt that pathologic diagnosis is the most accurate diagnosis for lung tumors. When possible, clinicians

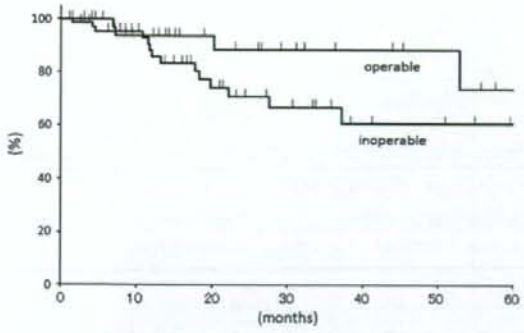

Fig. 3. Kaplan-Meier curve of overall survival rates for operable (n = 43) and inoperable (n = 72) patients. No statistically significant difference was found (p = 0.07) between two groups.

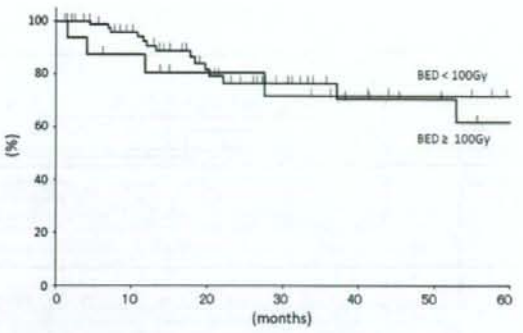

Fig. 4. Kaplan-Meier curve of overall survival rates for the patients with a biologic effective dose (BED) <100 (n = 17) and a BED ≥100 (n = 98). No statistically significant difference was found (p = 0.95) between the two groups.

should persuade patients to receive pathologic confirmation before SBRT and to receive surgical resection if they are operable. However, as we have observed in this retrospective study, for patients with poor respiratory function, pathologic confirmation of the small lung lesions is often difficult or life threatening and occasionally abandoned by pulmonologists and thoracic surgeons. Therefore, it is extremely important to find a subset of patients who would benefit from SBRT instead of the conventional strategy of watchful waiting or elective surgical resection.

In patients with clinically diagnosed lung cancer ≤20 mm in diameter, the 3-year survival rate was 89.8% in our series. Although the median follow-up is still short, the 5-year survival rate was projected to be 89.8% for these patients. Because of the very low complication rate for these patients, SBRT for inoperable patients highly likely to have Stage I lung cancer with tumors ≤20 mm in diameter may be justifiable. However, the excellent survival rates for those patients with tumors ≤20 mm may be partly caused by the inclusion of nonmalignant lesions in the radiation-treated patients. The clinical implications of the high local control rate depend on the accuracy of clinical/radiologic diagnosis for small lung lesions and are to be carefully evaluated in a prospective study.

Median follow-up period 14 months was relatively short, including 11 patients whose follow-up period was <4 months. However, 3- and 5-year survival data were not impacted so much by them because follow-up period of the other patients was much longer.

Onishi *et al.* reported that the patients treated with BED <100 Gy had a tendency to have worse clinical outcomes than those treated with larger dose in SBRT (1). In this study, there were only 17 patients who received BED <100 Gy. There was no significant difference in overall survival rates between those treated with BED <100 Gy and those treated with BED≥100Gy, probably because of the small number of the patients who received BED <100 Gy.

Improvement of clinical/radiologic diagnosis of small lung tumors is essential if SBRT is used for clinically diagnosed Stage I lung cancer. Before the introduction of FDG-PET, the percentage of benign diseases in the solitary lung nodules detected by plain chest X-ray or CT was reported to be 25% to 50%, which is obviously too high (9–12). However, improvement of imaging modalities has made it possible to diagnose small peripheral lung cancer much more precisely than before. There were recent reports that FDG-PET and PET/CT showed 88% to 96.8% sensitivity, 77% to 77.8% specificity, and 91.2% accuracy in diagnosis of primary lung cancer (13, 14). A combination of positive FDG-PET findings, enlargement of the nodule on CT image, and negative laboratory tests for worsening of inflammatory diseases would reduce the false-positive diagnosis of Stage I lung cancer. However, Nomori *et al.* reported that lung nodules that were <10 mm in size or that showed ground-glass opacity on CT image cannot be evaluated accurately by FDG-PET (15). Therefore, for solid round tumors ≤10 mm and those with ground-glass appearance, watchful waiting would be the preferable choice at present, and improvement in diagnostic imaging is warranted. In addition, even if small lung lesions are highly suggestive of primary lung cancer on clinical/radiologic examination, the possibility of small-cell lung cancer (SCLC), for which it is better to be given additional chemotherapy, cannot be excluded. Some tumor markers such as neuron-specific enolase or progastrin-releasing peptide are shown to have relatively high sensitivity and specificity for SCLC (16). Tumor marker screening has the potential to reduce the inclusion of SCLC, although the tumor size may be too small to detect marker elevation.

Recently video-assisted thoracoscopic surgery (VATS) for lung cancer has become a safe and common procedure. In comparison with open surgery, VATS is less invasive and is associated with less morbidity and mortality (17). However, a recent review showed that VATS still has a 3.3% to 13.4% complication rate for surgical biopsy and a 7.7% to 36.6% complications rate for lobectomy (17). In 567 patients with peripheral NSCLC ≤20 mm who were operable as evaluated by cardiopulmonary function tests and had no history of previously treated cancer, the complication rate was reported to be 6.6% for sublobar resection and 7.3% for lobar

resection with 1 operative death (18). In the present SBRT study, for patients with a peripheral lung tumor ≤20 mm who were often inoperable based on cardiopulmonary function tests and who could have a history of previously treated cancer, only 3.4% (2 of 58) experienced Grade 2 pulmonary complications and none experienced Grade 3 to 5 complications. Therefore, although the comparison of the complication between surgery and SBRT is difficult, SBRT can be regarded as a safer treatment than lobectomy using VATS and as safe as biopsy using VATS for patients with a tumor size ≤20 mm. On the contrary, for patients with a tumor size >20 mm, Grade 2, 3, and 5 pulmonary complications were observed in 8.8% (5 of 57), 5.3% (3 of 57), and 1.8% (1 of 57) of study patients, respectively. Because the risk of SBRT is not minimal for these patients, the indication of SBRT for clinically diagnosed Stage I lung cancer with a tumor >20 mm should be very carefully evaluated by members of the cancer board in each institution.

It is important to state that our study does not give any guidance for inoperable patients whose tumors are highly suggestive of benign lesions but that cannot be definitely determined not to be malignant, as this study looks only at those with tumors highly suggestive of malignant lesions. Patients with benign pulmonary lesion such as hamartoma, granulomatous inflammation, and focal fibrosis may require pathologic confirmation because these patients sometimes have tumors highly suggestive of benign lesions but that cannot be definitely determined not to be malignant. At present, it is obvious that VATS should be recommended for operable patients with tumors that are highly suggestive of benign lesions but that cannot be definitely determined not to be malignant, as VATS gives us pathologic confirmation.

CONCLUSION

In conclusion, in clinically diagnosed Stage I lung cancer patients with a tumor ≤20 mm in diameter, SBRT was reasonably safe in this retrospective study. The clinical implications of the high local control rate depend on the accuracy of clinical/radiologic diagnosis for small lung lesions and are to be carefully evaluated in a prospective study.

REFERENCES

1. Onishi H, Shirato H, Nagata Y, *et al.* Hypofractionated stereotactic radiotherapy (HypoFXSRT) for stage I non-small cell lung cancer: Updated results of 257 patients in a Japanese multi-institutional study. *J Thorac Oncol* 2007;2:S94–S100.
2. Uematsu M, Shioda A, Suda A, *et al.* Computed tomography-guided frameless stereotactic radiotherapy for stage I non-small cell lung cancer: A 5-year experience. *Int J Radiat Oncol Biol Phys* 2001;51:666–670.
3. Nagata Y, Takayama K, Matsuo Y, *et al.* Clinical outcomes of a phase I/II study of 48 Gy of stereotactic body radiotherapy in 4 fractions for primary lung cancer using a stereotactic body frame. *Int J Radiat Oncol Biol Phys* 2005;63:1427–1431.
4. Koto M, Takai Y, Ogawa Y, *et al.* A phase II study on stereotactic body radiotherapy for stage I non-small cell lung cancer. *Radiother Oncol* 2007;85:429–434.
5. Nyman J, Johansson KA, Hulten U. Stereotactic hypofractionated radiotherapy for stage I non-small cell lung cancer—mature results for medically inoperable patients. *Lung Cancer* 2006;51:97–103.
6. Onimaru R, Fujino M, Yamazaki K, *et al.* Steep dose-response relationship for stage I non-small-cell lung cancer using hypofractionated high-dose irradiation by real-time tumor-tracking radiotherapy. *Int J Radiat Oncol Biol Phys* 2008;70:374–381.
7. McGarry RC, Papiez L, Williams M, *et al.* Stereotactic body radiation therapy of early-stage non-small-cell lung carcinoma: Phase I study. *Int J Radiat Oncol Biol Phys* 2005;63:1010–1015.
8. Nishio T, Kunieda E, Shirato H, *et al.* Dosimetric verification in participating institutions in a stereotactic body radiotherapy trial for stage I non-small cell lung cancer: Japan clinical oncology group trial (JCOG0403). *Phys Med Biol* 2006;51:5409–5417.
9. Shaffer K. Role of radiology for imaging and biopsy of solitary pulmonary nodules. *Chest* 1999;116:519S–522S.
10. Libby DM, Henschke CI, Yankelevitz DF. The solitary pulmonary nodule: Update 1995. *Am J Med* 1995;99:491–496.
11. O'Reilly PE, Brueckner J, Silverman JF. Value of ancillary studies in fine needle aspiration cytology of the lung. *Acta Cytol* 1994;38:144–150.
12. Mack MJ, Hazelrigg SR, Landreneau RJ, *et al.* Thoracoscopy for the diagnosis of the indeterminate solitary pulmonary nodule. *Ann Thorac Surg* 1993;56:825–830; discussion 830–822.
13. Gould MK, Maclean CC, Kuschner WG, *et al.* Accuracy of positron emission tomography for diagnosis of pulmonary nodules and mass lesions: A meta-analysis. *J Am Med Assoc* 2001;285:914–924.
14. Jeong SY, Lee KS, Shin KM, *et al.* Efficacy of PET/CT in the characterization of solid or partly solid solitary pulmonary nodules. *Lung Cancer* 2008;61:186–194.
15. Nomori H, Watanabe K, Ohtsuka T, *et al.* Evaluation of F-18 fluorodeoxyglucose (FDG) PET scanning for pulmonary nodules less than 3 cm in diameter, with special reference to the CT images. *Lung Cancer* 2004;45:19–27.
16. Lamy P, Grenier J, Kramar A, *et al.* Pro-gastrin-releasing peptide, neuron specific enolase and chromogranin A as serum markers of small cell lung cancer. *Lung Cancer* 2000;29:197–203.
17. Solaini L, Prusciano F, Bagioni P, *et al.* Video-assisted thoracic surgery (VATS) of the lung: Analysis of intraoperative and postoperative complications over 15 years and review of the literature. *Surg Endosc* 2008;22:298–310.
18. Okada M, Koike T, Higashiyama M, *et al.* Radical sublobar resection for small-sized non-small cell lung cancer: A multicenter study. *J Thorac Cardiovasc Surg* 2006;132:769–775.

IOP PUBLISHING PHYSICS IN MEDICINE AND BIOLOGY

Phys. Med. Biol. 53 (2008) 7137–7150 doi:10.1088/0031-9155/53/24/009

Gating based on internal/external signals with dynamic correlation updates

Huanmei Wu[1], Qingya Zhao[2], Ross I Berbeco[3], Seiko Nishioka[4], Hiroki Shirato[5] and Steve B Jiang[6]

[1] Purdue School of Engineering and Technology, Indiana University School of Informatics, IUPUI, Indianapolis, IN, USA
[2] School of Health Sciences, Purdue University, West Lafayette, IN, USA
[3] Department of Radiation Oncology, Dana-Farber/Brigham and Womens Cancer Center and Harvard Medical School, Boston, MA, USA
[4] NTT East-Japan Sapporo Hospital, Sapporo, Japan
[5] Hokkaido University Graduate School of Medicine, Sapporo, Japan
[6] Department of Radiation Oncology, School of Medicine, University of California, San Diego, CA, USA

E-mail: hw9@iupui.edu and sbjiang@ucsd.edu

Received 13 May 2008, in final form 27 October 2008
Published 26 November 2008
Online at stacks.iop.org/PMB/53/7137

Abstract

Precise localization of mobile tumor positions in real time is critical to the success of gated radiotherapy. Tumor positions are usually derived from either internal or external surrogates. Fluoroscopic gating based on internal surrogates, such as implanted fiducial markers, is accurate however requiring a large amount of imaging dose. Gating based on external surrogates, such as patient abdominal surface motion, is non-invasive however less accurate due to the uncertainty in the correlation between tumor location and external surrogates. To address these complications, we propose to investigate an approach based on hybrid gating with dynamic internal/external correlation updates. In this approach, the external signal is acquired at high frequency (such as 30 Hz) while the internal signal is sparsely acquired (such as 0.5 Hz or less). The internal signal is used to validate and update the internal/external correlation during treatment. Tumor positions are derived from the external signal based on the newly updated correlation. Two dynamic correlation updating algorithms are introduced. One is based on the motion amplitude and the other is based on the motion phase. Nine patients with synchronized internal/external motion signals are simulated retrospectively to evaluate the effectiveness of *hybrid gating*. The influences of different clinical conditions on hybrid gating, such as the size of gating windows, the optimal timing for internal signal acquisition and the acquisition frequency are investigated. The results demonstrate that dynamically updating the internal/external correlation in or around the gating window will reduce false positive with relatively diminished treatment efficiency. This improvement will benefit patients with

0031-9155/08/247137+14$30.00

mobile tumors, especially greater for early stage lung cancers, for which the tumors are less attached or freely floating in the lung.

(Some figures in this article are in colour only in the electronic version)

1. Introduction

It is well known that respiration-induced tumor motion will degrade the effectiveness of radiation treatment (Bortfeld *et al* 2002, Jiang *et al* 2003). Gated radiotherapy is an advanced radiation treatment method for tumors with respiratory motion (e.g., Jiang 2006) since gated treatment holds promise to reduce the incidence and severity of normal tissue complications and to increase local control through dose escalation (Keall *et al* 2002). However, due to the reduced clinical tumor volume to planning target volume (CTV-to-PTV) margin, the success of gated treatment largely depends upon precise target localization in real time.

Generally, gated treatments use various surrogates to derive tumor position during real-time treatment, although recent efforts have been made to generate gating signals from direct localization of the tumor mass (Berbeco *et al* 2005, Cui *et al* 2007). Gating based on internal surrogates (i.e., *internal gating*), such as the gold markers implanted in or near a tumor in the real-time tumor-tracking radiation therapy (RTRT) system (Shirato *et al* 2000a), has satisfactory precision. However, marker implantation is invasive and radiation dose to patients from fluoroscopic marker tracking is a big concern. With many treatment fractions or long treatment duration of a single fraction, the accumulative imaging dose can be more than is clinically acceptable (Jiang 2006). Gating based on external surrogates (i.e., *external gating*), such as markers placed on the surface of the patients' abdomen for the real-time position management (RPM) respiratory gating system (Kubo and Hill 1996, Vedam *et al* 2001) is easy, noninvasive, and radiation dose free. However, the precision is often less satisfactory (Berbeco *et al* 2005, Ionascu *et al* 2007, Seppenwoolde *et al* 2007).

Therefore, it is natural to combine the advantages of both internal and external gating. The goal is to reduce the internal imaging frequency by utilizing the external marker together with the internal marker. For effective gated treatment, updating the internal/external correlation in real time during treatment is required since it improves the confidences of external gating. One way of integrating internal/external markers has been explored on the CyberKnife System (Murphy 2004, Schweikard *et al* 2000). Markers on the patients' abdomen are constantly tracked and used to derive tumor positions. X-ray images are taken periodically (every 30 or 60 s) to re-calibrate the internal/external correlation. There is no correlation updating during a treatment beam. Kanoulas *et al* (2007) proposed an algorithm to update internal/external correlation with a fixed updating frequency (such as 10 Hz). Both methods acquire internal tumor positions at a fixed frequency and internal motion acquisition can occur at any stage of a breathing cycle. They are suitable for radiation treatment with beam tracking. However, they are not optimized for gated treatment.

We propose a *hybrid gating* technique which integrates the external and internal signals specially optimized for respiratory gating. This approach addresses some special concerns of gated treatment. For example, it ensures accurate internal/external correlation in or near the gating window although the correlation outside the gating window is not guaranteed. This paper will introduce two dynamic correlation updating algorithms optimized for hybrid gating with low-updating frequency ($\leqslant$0.2 Hz).

2. Methods and materials

2.1. Materials

We have retrospectively evaluated our proposed hybrid gating based on patient data collected at the Nippon Telegraph and Telephone Corporation (NTT) Hospital in Sapporo, Japan (Berbeco *et al* 2005). The 3D internal signals were acquired by fluoroscopic tracking of the implanted fiducial markers in or near the tumor with a Mitsubishi real-time tumor-tracking radiation therapy (RTRT) system (Shirato *et al* 2000a). The external signals are one-dimensional relative movement of patient abdominal surface, acquired through an external surrogate using the AZ-733V external respiratory gating system integrated with the RTRT system. The synchronized internal and external signals are gathered at 30 Hz throughout a treatment.

Nine lung patients with multiple ($\geqslant$4) treatment sessions are studied, of which the superior–inferior (SI) tumor motion is more than 7 mm. Only SI motion is studied in our hybrid gating since it is the most significant motion. Together, there are 154 treatment sessions for these nine patients. Detailed information about the patients studied has been introduced by other investigators (Berbeco *et al* 2005, Ionascu *et al* 2007).

2.2. Effects of correlation changes over gating treatment

Most patients exhibit one or more unsynchronized changes of amplitude variations, phase shifts and baseline drifts between internal and external motion signals. Examples are demonstrated in figure 1, which also shows the distinctive correlation patterns for the same patient at different times. The changes of internal/external correlation have great effects over gated treatment, which are illustrated in figure 2. The false positive is when the radiation beam is on while the tumor is out of the gating window. During a false positive, more radiation dose goes to healthy tissue and critical structures than was planned. The false negative is when the radiation beam is off while the tumor is in the gating window. From the point of clinical practice, a false positive is more serious than a false negative. Thus, the primary concern is to promote gating accuracy while maintaining an acceptable gating efficiency.

2.3. Gated treatment based on updated internal/external correlation

The proposed hybrid gating is a two-step procedure: *correlation initialization* (a pre-treatment step) and *correlation adjustment* (an online treatment step), which are introduced below:

(i) *Correlation initialization.* Before gated treatment, both the internal and external motion signals are acquired at high frequency (30 Hz for our test data) for a few breathing cycles. These high-frequency pre-treatment data will be applied to build the initial internal/external correlation. For the simulation presented in this paper, the training data are the first three full breathing cycles (a breathing cycle starts from the beginning of an exhale and ends at the end of the immediate next inhale). A variety of correlation algorithms can be used in this step. We have used the min max normalization (Han and Kamber 2006) in which the internal motion signal will not change while the external signal is scaled as follows:

$$e'(t) = \frac{(e(t) - e_{\min}) \cdot (x_{\max} - x_{\min})}{e_{\max} - e_{\min}} + x_{\min}, \tag{1}$$

where $e(t)$ and $e'(t)$ are the original and the correlated external signals, respectively, $e_{\max}$ and $e_{\min}$ (or $x_{\max}$ and $x_{\min}$) are the maximum and minimum values of the original external (or internal) signal.

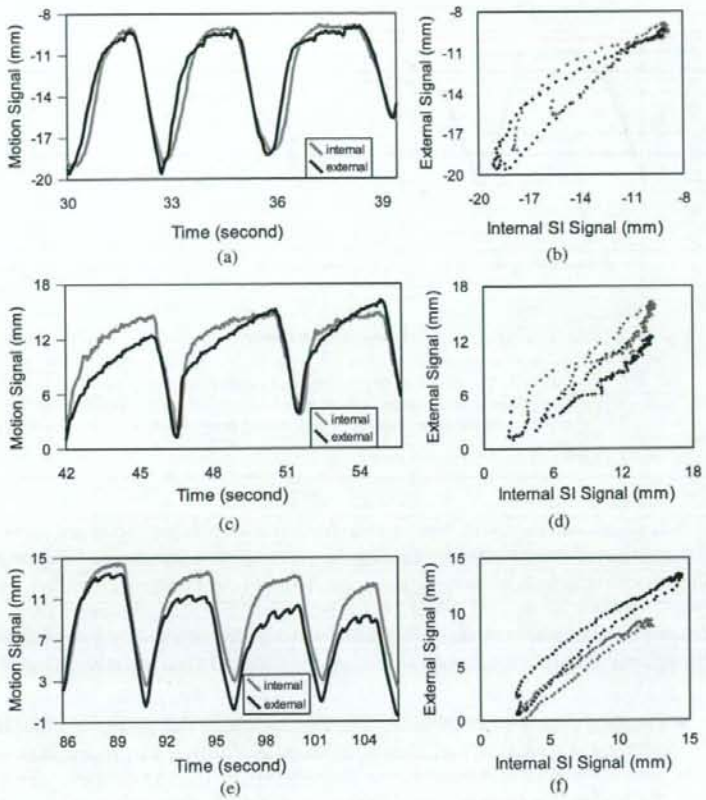

Figure 1. Internal/external motion signals and correlation patterns with phase shift (a) and (b), with baseline drift and amplitude variation (c) and (d) and with combination of phase shift, baseline drift and amplitude variation (e) and (f). The figures on the right (b), (d) and (f) display the internal/external correlations of the first (dark black dots) and last breathing cycles (gray dots) of each corresponding pair of motion signals.

(ii) *Correlation adjustment.* Due to changes of internal/external correlation over time, the initial correlation may not be a good reflection of the correlation during treatment. Updating the correlation in real time is necessary to accurately derive the internal tumor location based on the external signal. When an updating event occurs at t_i, the internal position is acquired, denoted as $x(t_i)$. Any external signal after t_i will be calculated according to the following equation:

$$e'(t) = e'_{\text{pre}}(t) - [e'_{\text{pre}}(t_i) - x(t_i)], \tag{2}$$

where $e'_{\text{pre}}(t)$ and $e'_{\text{pre}}(t_i)$ are the correlated external signals, at times t and t_i respectively, calculated based on the previous active correlation at t_i. Equation (2) will be the active correlation after t_i until the next updating event.

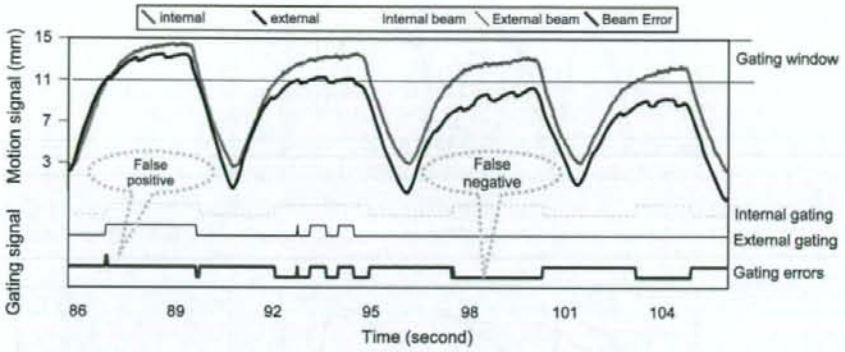

Figure 2. The effects of internal/external correlation changes over gated treatment. The internal gating shows the beam on and off based on internal motion signal while the external gating is based on the correlated external signal. Gating errors show the differences of internal and external gating.

It is critical to update the internal/external correlation when the tumor moves into the gating window to improve the effectiveness of gated treatment (supporting results are demonstrated in figure 6 and section 3.1). A successful updating algorithm needs to address two important issues: (*i*) *when* is the best time to update the correlation and (*ii*) *how* frequently an update is needed. This paper will describe two updating algorithms to determine the optimal updating time: one is based on the amplitude and the other is based on the phase.

- *Updating based on amplitude.* For this approach, the gating window is divided into different percentages based on amplitude, as illustrated in figure 3(a). One of these percentage lines is defined as the updating trigger line. Once the external signal passes the trigger line from below to above, an updating event will be triggered. Figure 3(a) demonstrates the corresponding updating events at the 0%, 25% and 50% percentage lines, for which the updating frequency is one update per breathing cycle. The amplitude-based updating is simple and straightforward. However, there can be no updating point for some breathing cycles. For instance, there is no update for the 50% percentage line for the first breathing cycle since the external signal never passes the 50% line in this breathing cycle. The worst case is that the external signal is always below the predefined amplitude percentage line. In this case, there will be no updates at all.
- *Update based on phase.* A piecewise linear representation (PLR) of respiratory motion (Wu *et al* 2004) decomposes a normal breathing cycle into three states: exhale (EX), end-of-exhale (EOE) and inhale (IN). The gating window (generally at the EOE state) for the external signal is divided into different phases based on the duration as demonstrated in figure 3(b). When the external signal passes the predefined triggering phase, the updating event will be activated. The phase-based algorithm ensures there is one updating point for every breathing cycle.

2.4. Gating window determination

We propose a clinical oriented approach to determining the gating window position, as shown in figure 4. The peak points at the EOE states are identified and the mean position of these peak

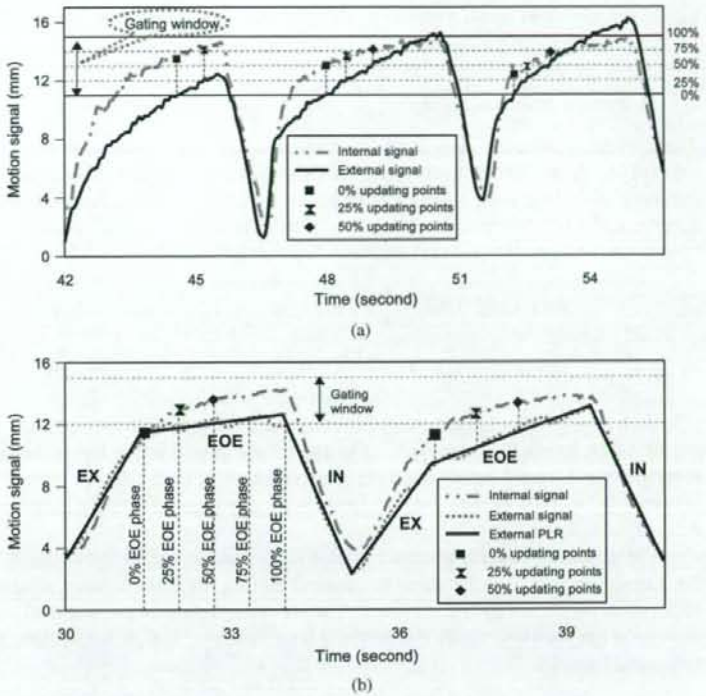

Figure 3. Two algorithms for online correlation adjustment during radiation treatment: (a) based on amplitude inside a gating window and (b) based on the phase of a piecewise linear model of external signal.

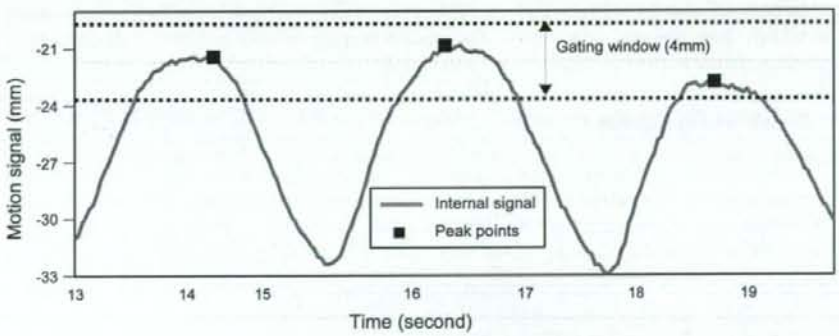

Figure 4. Determination of a gating window position based on the training data sets. The average of the peak points at the end-of-exhale is the center of the gating window.

points will be the middle position of the gating window. The simulation results presented in this paper use the first three breathing cycles to calculate the gating window position. Various

gating window sizes (from 2 mm to 6 mm) will then be simulated to assess the effect of gating window sizes on gated treatment.

2.5. *Evaluation of hybrid gating*

Three metrics, namely, *duty cycle*, *target coverage* and *residual motion*, are defined to retrospectively evaluate the outcomes of hybrid gating. Assuming t_0 is the total treatment duration, including both beam-on and beam-off time, t_1 is the beam-on time based on a specific updating algorithm (true positives plus false positives), and t_2 is the correct beam-on time (true positive), the two metrics are defined as follows:

$$\text{duty cycle (DC)} = \frac{t_1}{t_0} \cdot 100\%. \tag{3}$$

$$\text{target coverage (TC)} = \frac{t_2}{t_1} \cdot 100\%. \tag{4}$$

Both false positives and false negatives are considered in the two metrics. The more false negatives the lower the duty cycle. The more false positives the lower the target coverage. Ideally, a good hybrid gating algorithm should result in high DC and high TC. If a tradeoff between DC and TC is required, the focus is on improving TC while maintaining the DC at an acceptable level.

The residual motion is used to evaluate the statistical variability of the motion signals in the gating window. To calculate the residual motion, first, the motion position is classified either in or outside a gating window. The residual motion is the standard deviation of the corresponding motion signal inside the gating window, which is calculated based on the following formula:

$$\text{residual motion} = \sqrt{\left(x_i - \frac{\sum x_i}{n-1}\right)^2}, \tag{5}$$

where x_i is the motion signal inside a gating window of either the original signals or the updated signals.

The residual error between the internal target position and the edge of the gating window for all false positives is also measured. The relative average distance and total distance of false positives during a treatment fraction are calculated.

3. Results and discussion

The differences of hybrid gating with or without dynamic online adjustment of internal/external correlation are illustrated in figure 5. The updating algorithm is based on the piecewise linear model (PLR) at the 0% phase. It can be observed from the figure that both false positives and false negatives have been reduced for this specific patient. Similar results have been observed in the amplitude-based updating algorithm.

3.1. *Results on the effects of updating timing*

The optimal timing to update the internal/external correlation is an important issue for an updating algorithm. Figure 6 demonstrates the timing effects using amplitude-based updating algorithm. Nine timing options inside or outside the gating window at the exhale stage are illustrated in figure 6(a). The changes of target coverage (TC) and the duty cycle (DC) for one patient and the average for all the patients are illustrated in figures 6(b) and (c).

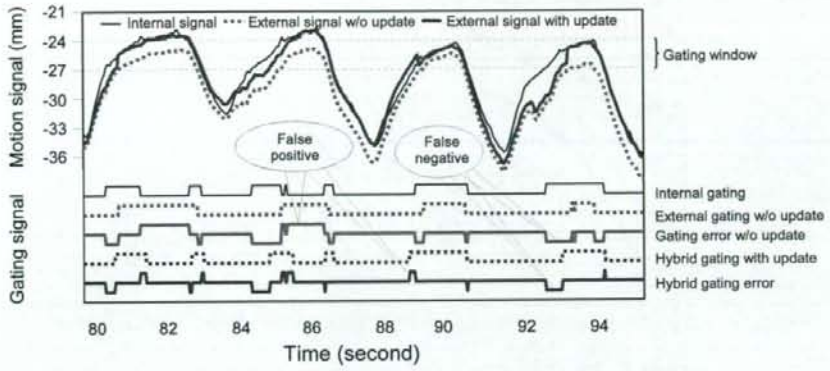

Figure 5. The outcome of hybrid gating with online adjustment of internal/external correlation based on the phase, along with the corresponding gating signals and gating errors.

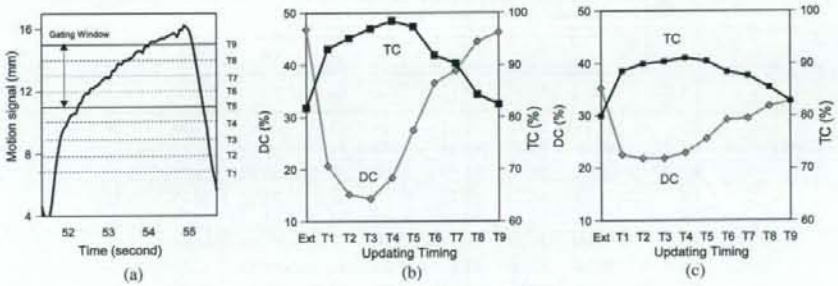

Figure 6. The timing effects on target coverage (TC) and duty cycle (DC) for amplitude-based updating where the updating frequency is once every cycle and the gating window size is 4 mm. (a) Illustration of the different updating points on the exhale state based on amplitude (b) the DC and TC changes for a specific patient averaged over 23 treatment sessions, and (c) the DC and TC changes averaged over 160 treatment sessions of nine patients.

The figures showed that hybrid gating with online correlation adjustment improves target coverage (TC), however it also brings down the duty cycle (DC). This is true at different timings. The improvement of TC is most prominent when the tumor moves into the gating window (updating timing T3, T4 and T5), i.e., near the transition points from exhale to end-of-exhale state. The improvement decreases as the updating timing is away from (both before or after) the transition points. The reduction of DC is significant in the exhale state but does not change too much in the end of exhale state.

The detailed effects of updating timings inside the gating window on gated treatments for nine patients are summarized in table 1. The phase-based updating yields similar results to the amplitude-based updating. A common observation from the table is that correlation updating will improve the target coverage but decrease the duty cycle inside the gating window. In addition, for most patients, updating at the earlier stage of the gating window shows greater improvements in the target coverage. In the following, we will focus on the updating results

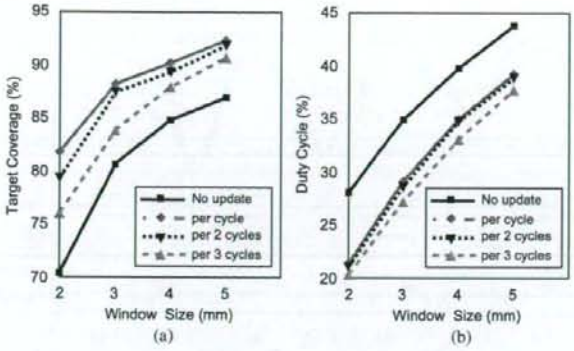

Figure 7. The effects of updating frequency on target coverage (TC) and duty cycle (DC) for amplitude-based updating, where the updating frequencies range from one update for every breathing cycle to one update for every three breathing cycles.

Table 1. The timing effects inside a gating window for amplitude-based updating of nine patients where gating window is 3 mm and updating frequency is once every cycle.

	TC (%)				DC (%)			
Patients	ext	T5	T6	T7	ext	T5	T6	T7
P1	75.39	90.46	90.02	85.40	21.39	20.42	19.59	16.28
P2	81.66	92.52	83.96	86.64	41.85	18.72	35.13	36.34
P3	78.93	94.48	90.86	89.78	40.77	20.07	29.71	30.86
P4	78.63	88.20	87.10	87.75	22.00	21.55	20.58	19.78
P5	77.53	96.52	93.00	90.47	33.19	21.28	22.89	22.58
P6	54.09	70.53	74.71	71.13	18.61	14.80	14.53	17.11
P7	55.76	75.00	82.18	77.32	40.36	11.02	17.35	19.83
P8	80.64	88.19	82.91	81.01	34.92	29.11	29.46	30.53
P9	77.56	84.36	87.66	85.59	19.93	23.11	21.79	19.89

on updating at lower edge of the gating window, i.e., the updating timing option T5 as shown in figure 6(a).

3.2. Results on the effects of updating frequencies

The choice of the updating frequency can be a challenging issue for real-time dynamic correlation updating. The effects of updating frequencies are demonstrated in figure 7 and table 2 for amplitude-based updating, where the updating frequencies range from one update per breathing cycle to one update every three breathing cycles. The average differences between updating every cycle and every two cycles are $1.65 \pm 0.26\%$ for TC (column $TC_1 - TC_2$) and $0.18 \pm 0.14\%$ for DC (column $DC_1 - DC_2$). The differences between updating every cycle and every three cycles are $4.98 \pm 1.34\%$ for TC and $0.63 \pm 0.55\%$ for DC. One notable exception is patient 9, who has extremely irregular external motion signal with erratic baseline shift, large amplitude oscillation, and frequency changes. Although its TC has improved with low-updating frequency, its DC has decreased. Similar results have been observed for the phase-based updating. The higher the frequency at which the updating

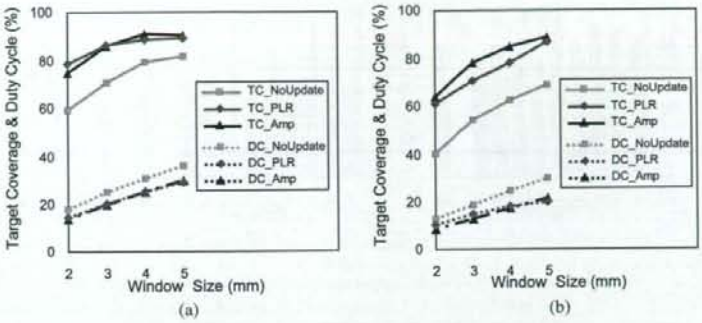

Figure 8. The effects of gating window sizes on target coverage (TC) and duty cycle (DC) for different external gating approaches (without updating, or updating based on amplitude or PLR): (a) for a patient with regular motion and (b) for a patient with erratic motion. The updating frequency is once per breathing cycle at 0% amplitude or EOE phase.

Table 2. The effects of the updating frequencies on amplitude-based updating where gating window size is 3 mm and the frequencies are one update per one (DC_1 and TC_1) or two (DC_2 and TC_2) or three (DC_3 and TC_3) breathing cycles.

	TC	(%)	DC	(%)
Patients	$TC_1 - TC_2$	$TC_1 - TC_3$	$DC_1 - DC_2$	$DC_1 - DC_3$
P1	2.62	14.36	−0.41	0.10
P2	0.60	4.45	0.17	−2.17
P3	1.03	4.78	−0.09	−3.25
P4	2.06	4.07	0.27	0.11
P5	1.60	3.97	0.23	−1.14
P6	1.92	3.43	−0.19	0.66
P7	2.57	0.43	0.94	−1.24
P8	0.79	4.35	0.55	1.92
P9	1.08	−9.51	0.46	−11.37
Average (P1 to P9)	1.65 ± 0.26	4.98 ± 1.34	0.18 ± 0.14	-0.63 ± 0.55

is performed, the better the target coverage (TC). The effects of updating frequencies are relatively small for DC.

3.3. Results on the effects of gating window sizes

The effects of gating window sizes on the efficacy of gated treatments have been analyzed and the results of two representative patients are illustrated in figure 8. Figure 8(a) shows a patient with regular motion and figure 8(b) shows one with quite irregular motion. The target coverage (TC) and duty cycle (DC) are compared among three gating approaches: external gating without correlation updating, hybrid gating with amplitude-based updating, and hybrid gating with phase-based updating. Generally, larger gating windows result in better target coverage and higher duty cycle. The duty cycle of most patients is $\geqslant$20% when the gating window $\geqslant$3mm.

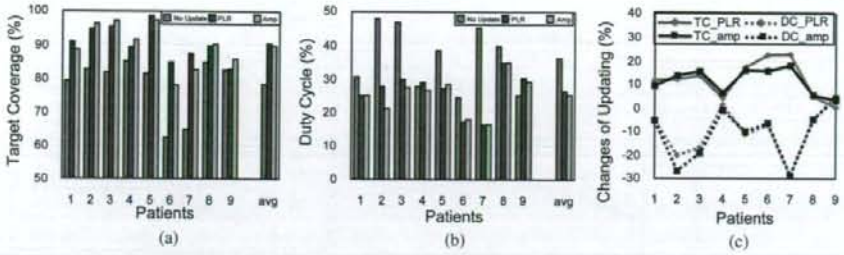

Figure 9. The results of dynamic correlations updating for gated treatments: (a) target coverage and (b) duty cycles and (c) changes of TC and DC induced by dynamic correlation updating. The 'avg' shows the TC and DC averaged over all patients.

The results show the impact of gating window size, which is restricted by the process of treatment planning. Most gated treatments use a gating window with fixed size and fixed position determined by the treatment planning process. Further investigation is needed to apply the proposed approach under clinical conditions, where the restriction of the treatment planning process will be taken into consideration.

3.4. Evaluation of dynamic updating on gated treatments

Figure 9 summarizes the target coverage (TC) and duty cycle (DC) for each patient, averaged over the whole treatment course. With dynamic updating, either amplitude- or phase-based updating, the target coverage is improved, notably for six patients (10% more than without updating), moderately for two patients, and slightly for one (patient 9 who has erratic motion). The average increase in TC, averaged over all patients, is 12% for phase-based updating and 11% for amplitude-based updating. However, the duty cycle has diminished with internal/external correlation updating (except patient 4 increases the DC by 1.3% for phase-based updating). The average decrease in DC is 10% for phase-based updating and 11% for amplitude-based updating.

Thus, applying either updating method will improve the outcome of gated treatment, although the phase-based approach showed slightly better performance than the amplitude-based approach for most patients. Target coverage demonstrates the precision of delivered radiation dose to the patients while the duty cycle indicates the duration of a gated treatment. Lower target coverage means more radiation dose to the healthy tissue or critical structures. From the view of clinical applications, as long as the duty cycle satisfies a certain threshold (such as at least 20%), the improvement of target coverage has great impact for precise radiation treatment.

3.5. Residual motion in the gating window

The residual motion, which is the standard deviation of the corresponding motion signal in the gating window, of two patients is illustrated in figure 10. One patient has regular motion and the other has irregular motion. It is shown that the residual motion has no significant difference whether the internal/external correlations are dynamically updated or not. Thus, our updating algorithms do not create large dispersion of the motion signals in the gating window.

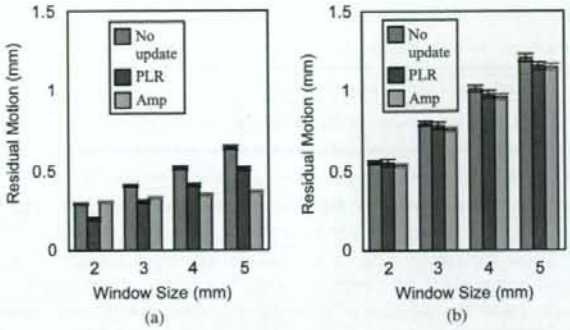

Figure 10. The residual motion in the gating window of the accumulative treatment signals: (a) the residual motion of a patient with regular motion and (b) the residual motion of a patient with irregular motion.

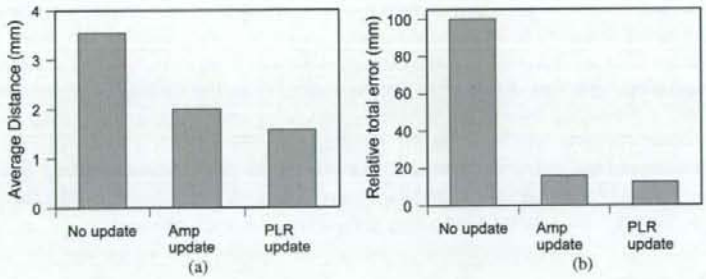

Figure 11. The false positive errors for a treatment session of a specific patient using different correlation approaches: (a) the average distance and (b) the total accumulative distances between the correlated tumor position and true internal position.

The errors between the internal target position and the edge of the gating window for all false positives are calculated. The average distances of a treatment fraction, either with or without update, are illustrated in figure 11(a), which showed that dynamic correlation updating reduced the residual error. The relative accumulative errors are demonstrated in figure 11(b), where the error without update is normalized to 100. For this treatment fraction, the relative accumulative errors with updates are less than 20 mm. One reason is that dynamic correlation updates reduce the false positive rate.

4. Summary

Two internal/external correlation updating algorithms have been proposed in this paper. One is based on the amplitude percentages in the gating window and the other is based on the phases of the end-of-exhale state (which usually is the gating window) from a piecewise linear representation (PLR) of motion signal. Comprehensive evaluation of gated treatment has been performed to test the effects of altered updating frequency, various gating window sizes, and

different updating timings for both amplitude- and phase-based updating approaches. Several metrics, including target coverage, duty cycle, residual motion in the gating window, residual error for all false positives, are defined to evaluate gated treatment.

The results showed that dynamic correlation updating is necessary for the success of gated radiation treatment. Moreover, gated treatment has high requirements for the timing of correlation updates, i.e., correlation updating near the gating window entry point improves more for the average target coverage, with some sacrifice of treatment efficiency. This is the major difference between our updating algorithms and other correlation updating methods (Kanoulas *et al* 2007). One update per breathing cycle (~0.2 Hz for internal imaging) is acceptable for most regular treatments with improved target coverage. For long lasting treatments, internal imaging can be further reduced by a factor of two, i.e., one update every two breathing cycles, with the sacrifice of a couple of percentages of target coverage (1.65%). Compared to the RTRT system with an internal imaging rate of 30 Hz, our approach has reduced the internal imaging dose more than 150 times. The residual errors in the gating window or for all false positive showed that our updating algorithms reduce residual motion and lower false positive rate.

Further investigation is being carried out to study gating based on updated internal/external signals in a clinical environment. For example, one direction is to integrate advanced features, such as the estimation of motion uncertainties and phase discrepancies during internal imaging, and the impact of motion hysteresis, into the correlation updating algorithm. Another direction is the simulation of gating during a real-time treatment with motion prediction by considering the system delay and imaging rate (Sharp *et al* 2004). Yet another direction is to integrate the updating algorithms to dynamically change the sizes and positions of the gating window under the restrictions of treatment planning system. It will be very useful for patients with irregular motion, especially with baseline drift. In addition, more precise evaluation metrics for gating are under active exploration.

References

Berbeco R I, Mostafavi H, Sharp G C and Jiang S B 2005a Towards fluoroscopic respiratory gating for lung tumours without radiopaque markers *Phys. Med. Biol.* **50** 4481–90

Berbeco R I, Nishioka S, Shirato H, Chen G T Y and Jiang S B 2005b Residual motion of lung tumours in gated radiotherapy with external respiratory surrogates *Phys. Med. Biol.* **50** 3655–67

Bortfeld T, Jokivarsi K, Goitein M, Kung J and Jiang S B 2002 Effects of intra-fraction motion on IMRT dose delivery: statistical analysis and simulation *Phys. Med. Biol.* **47** 2203–20

Chui C S, Yorke E and Hong L 2003 The effects of intra-fraction organ motion on the delivery of intensity-modulated field with a multileaf collimator *Med. Phys.* **30** 1736–46

Cui Y, Dy J G, Sharp G C, Alexander B and Jiang S B 2007 Robust fluoroscopic respiratory gating for lung cancer radiotherapy without implanted fiducial markers *Phys. Med. Biol.* **52** 741–55

Han J and Kamber M 2000 *Data Mining Concepts and Techniques* 2nd edn (New york: Morgan Kaufmann)

Ionascu D, Jiang S B, Nishioka S, Shirato H and Berbeco I R 2007 Internal–external correlation investigations of respiratory induced motion of lung tumors *Med. Phys.* **34** 3893–903

Jiang S B 2006 Radiotherapy of mobile tumors *Semin. Radiat. Oncol.* **16** 239–48

Jiang S B, Pope C, Aljarrah K M, Kung J, Bortfeld T and Chen G T Y 2003 An experimental investigation on intra-fractional organ motion effects in lung IMRT treatments *Phys. Med. Biol.* **48** 1773–84

Kanoulas E, Aslam J A, Sharp G C, Berbeco R I, Nishioka S, Shirato H and Jiang S B 2007 Derivation of the tumor position from external respiratory surrogates with periodical updating of the internal/external correlation *Phys. Med. Biol.* **52** 5443–56

Keall P J, Kini V R, Vedam S S and Mohan R 2002 Potential radiotherapy improvements with respiratory gating *Australas. Phys. Eng. Sci. Med.* **25** 1–6

Korreman S, Christensson J, Mostafavi H, Loo B, Le Q and Boyer A 2007 Predictability of lung tumor motion based on external marker monitoring: linear and non-linear modelling *Proc. ICCR*

Kubo H D and Hill B C 1996 Respiration gated radiotherapy treatment: a technical study *Phys. Med. Biol.* **41** 83–91

Murphy M J 2004 Tracking moving organs in real time *Semin. Radiat. Oncol.* **14** 91–100
Schweikard A *et al* 2000 Robotic motion compensation for respiratory movement during radiosurgery *Comput. Aided. Surg.* **5** 263–77
Seppenwoolde Y, Berbeco R I, Nishioka S, Shirato H and Heijmen B 2007 Accuracy of tumor motion compensation algorithm from a robotic respiratory tracking system: a simulation study *Med. Phys.* **34** 2774–84
Sharp G C, Jiang S B, Shimizu S and Shirato S 2004 Prediction of respiratory tumour motion for real-time image-guided radiotherapy *Phys. Med. Biol.* **49** 425–40
Shirato H *et al* 2000 Four-dimensional treatment planning and fluoroscopic real-time tumor tracking radiotherapy *Int. J. Radiat. Oncol. Biol. Phys.* **48** 1187–95
van Herk M 2004 Errors and margins in radiotherapy *Semin. Radiat. Oncol.* **14** 52–64
Vedam S S, Keall P J, Kini V R and Mohan R 2001 Determining parameters for respiration-gated radiotherapy *Med. Phys.* **28** 2139–46
Wu H, Sharp G, Salzberg B, Kaeli D, Shirato H and Jiang S 2004 A finite state model for respiratory motion analysis in image guided radiation therapy *Phys. Med. Biol.* **49** 5357–72